Advances in Environmental Technology 11(1) 2025, 75-90.

Iranian Reasearch Organization for Science and Technology (IROST)

Advances in Environmental Technology

Journal home page: https://aet.irost.ir

Green synthesis of ZIF-8 nanoparticles for the simultaneous removal of Cd (II) and Sb (III) from contaminated wastewater

Pari Soltani[a], Mozhgan Zakeri*[a], Abdolreza Samimi[a], Azadeh Agah[b]

[a]Department of Chemical Engineering, Faculty of Engineering, University of Sistan and Baluchestan, Zahedan, Iran

[b]Department of Mining Engineering, Faculty of Engineering, University of Sistan and Baluchestan, Zahedan, Iran.

ARTICLE INFO

Document Type:
Research Paper

Article history:
Received 14 June 2024
Received in revised form
25 November 2024
Accepted 3 December 2024

Keywords:
Antimony and Cadmium Adsorption
Green Synthesis Wastewater Treatment
ZIF-8 Nanoparticles

ABSTRACT

Researching efficient and green methods for removing toxic heavy metals from contaminated environments is of paramount importance. In this study, ZIF-8 nanoparticles were successfully synthesized at ambient temperature and pressure using a non-toxic water solvent. The synthesized nanoparticles underwent characterization through Brunauer-Emmett-Teller (BET), X-ray powder diffraction (XRD), Fourier transform infrared spectroscopy (FTIR), and field emission scanning electron microscope (FESEM) analysis, followed by their application in the simultaneous adsorption of Sb (III) and Cd (II) from aqueous solutions. The thermodynamic behavior and adsorption kinetics of the prepared nanosorbent were also investigated. The kinetic data for cadmium and antimony adsorption on ZIF-8 nanoparticles exhibited a good fit with a pseudo-second-order model. The impact of pH on the adsorption capacity of synthesized nanoparticles for metal removal was evaluated. At T= 15◦C and pH 6.0, the maximum adsorption capacity of ZIF-8 nanoparticles was obtained: 31.8 mg·g^(-1) for Cd (II) and 87.68 mg·g^(-1) for Sb (III). The higher removal percentage for Sb (III) compared to Cd (II) might be because the ionic radius of antimony is smaller compared to cadmium, and its electronegativity is higher. The results demonstrated that ZIF-8 nanoparticles prepared through a facile and green method have the potential to serve as suitable adsorbents for the simultaneous uptake of cadmium and antimony from the environment.

1. Introduction

Nowadays, one of the most significant challenges societies face in environmental protection is the purification of polluted water and wastewater [1, 2]. Heavy metals are a hazardous pollutant found in water and wastewater [3]. The presence of excessive amounts of heavy metals in water is a consequence of societal industrialization and increased human activities [4-6]. Wastewater produced by industries such as mining [7-9], agriculture [10], textile [11, 12], tanning [13, 14], and dyeing [15, 16] contains significant amounts of

*Corresponding author Tel.: +98 9159022595
E-mail: m_zakeri@eng.usb.ac.ir
DOI: 10.22104/AET.2024.6938.1901

heavy metals, including Cd, Cu, Sb, Cr, Pb, Tl, Hg, which are often released into the environment without proper treatment. While heavy metals occur naturally in water, soil, and even in living organisms, their excessive levels are toxic to natural ecosystems and threaten human and organism health [17, 18]. In recent years, the substantial increase in wastewater production from Cu, Au, and Sb mines due to extensive mining activities has resulted in high concentrations of antimony and cadmium in the environment, raising concerns internationally. Wastewater from gold and antimony mining is an important source of contamination with various heavy metals, especially cadmium and antimony [19, 20]. Both Cd and Sb, even in small amounts, can adversely affect vital organs such as the liver, kidneys, lungs, and even the brain of humans and other living beings due to their toxicity and bioaccumulation in microorganisms [21-23]. According to the World Health Organization (WHO) guidelines, the maximum permissible concentrations for Sb and Cd in drinking water are respectively 5 μg. L-1 and 3 μg. L-1, due to their high toxicity [21, 24].

Various methods have been employed to eliminate metal ions from the ambiance, categorized into physicochemical and biological processes. Physicochemical methods include surface adsorption, flocculation, filtration, ion exchange resins, etc.; common biological methods include microremediation and phytoremediation [25-27]. Physicochemical methods are typically more straightforward and cost-effective compared to biological methods. Among these methods, surface adsorption has garnered significant attention. This approach utilizes solid materials with high porosity as adsorbents. Fortunately, a wide variety of adsorbents are available today [28]. Over time, advanced adsorbents such as CNTs [29], polymeric adsorbents [30, 31], and bi-metal oxide composites [32, 33] have gradually replaced traditional adsorbents like silica gels and activated carbon [34]. Metal-organic frameworks (MOFs) are a group of advanced adsorbents composed of metal ions and organic materials [35]. Their unique features, such as tunable porosity and high specific surface area, make them excellent candidates for removing various contaminants, particularly heavy metals, from industrial wastewater [36, 37]. MOFs are typically prepared through solvothermal and hydrothermal processes, which require high temperatures and pressures using organic solvents [38]. However, organic solvents are often expensive, toxic, and challenging to remove from the resulting MOFs. In recent years, a serious focus on environmental protection has given more attention to synthesizing MOFs at ambient temperature and pressure using non-toxic solvents. Zeolitic imidazolate frameworks (ZIFs) are a subfamily of MOFs. The structure of ZIFs is analogous to aluminosilicate zeolites, thus combining the advantages of both MOFs and natural zeolites. ZIF-8, with sodalite (SOD) topology, is a type of ZIFs with excellent unique properties such as ultrahigh porosity and specific surface area, thermal stability, and easy preparation. Due to these remarkable properties, ZIF-8 nanosorbent can be a good candidate for purification applications, especially for removing heavy metals from polluted waters [39, 40]. The successful application of ZIF-8 synthesized by different methods for removing the heavy metals As+3 and As+5 [41, 42], Pb+2 [43], Ni+2 [44], Cu+2 [45, 46], and Cr +6 [47] has been reported. There are not many studies among them in which ZIF-8 has been synthesized using green methods [41, 42]. Additionally, few fundamental studies have yet been carried out on the adsorption capacity of ZIF-8 MOF for the simultaneous removal of some heavy metal ions. Ling Hu et al. [48] investigated the simultaneous removal of Mn (II), Cu(II), and Cd(II) using ZIF-8 adsorbent. Their results demonstrated that ZIF-8 adsorbed heavy metal ions in the following order: Cu (II) > Mn (II) > Cd (II). Longwei Yin et al. [49] evaluated simultaneous adsorption of As (III) and As (V) from mining wastewater using ZIF-8 embedded with iron nanoparticles. Their experimental studies revealed that removal efficiencies were 99.9% and 71.2% for As (III) and As(V) ions, respectively.

Meanwhile, there is currently a high demand for new absorbents that do not cause environmental pollution during their production and have a high absorption capacity for various types of heavy metals in wastewater. To the best of the authors' knowledge, among all the research using ZIF-8 for water treatment, especially the removal of heavy metals, no sample of this adsorbent has been

developed that is both synthesized using a green method and can simultaneously adsorb two different heavy metals with an acceptable adsorption capacity. In this study, ZIF-8 nanoparticles were synthesized using a green and facile method at ambient pressure and temperature, utilizing water as the solvent. The prepared nanoparticles were characterized through FESEM, XRD, energy dispersive X-ray (EDX), and FTIR analysis. The thermodynamic behavior and kinetic models for the simultaneous adsorption of cadmium and antimony were investigated. The influence of pH on the removal capacity of the synthesized nanoparticles was assessed. The results provide a good understanding of the high capacity of ZIF-8 MOF for removing heavy metals from water environments.

2. Materials and methods

2.1. Materials

The $Zn(NO_3)_2$ (99%), NaOH (99%), $Cd(NO_3)_2$, and $SbCl_3$ standard solutions of 1000 mg. L^{-1} were purchased from Merck; the 2- methylimidazole ($C_4H_6N_2$, 99%) was supplied by Sigma Aldrich. All materials were used as obtained without additional treatment. Demineralized water was used in all experiments.

2.2. ZIF-8 green synthesis

ZIF-8 nanoparticles were prepared using the procedure described in reference [41], with water as the solvent at room temperature. Typically, 0.9 gr of $Zn(NO_3)_2$ and 22.7 gr 2-methylimidazol were separately dissolved in 8 and 89 cc of deionized water, respectively. The solutions were mixed (410 rpm, 5 min) with the molar ratio of cadmium/antimony: Hmim: H_2O equal to 1:90:1800 at room temperature (~15 ±2°C) (Figure 1a). The synthesized nanoparticles were separated using an ultrasonic bath and centrifugation (7500 rpm, 30 min). After washing and drying (80◦C, 24 h) (Figure 1b), the obtained product was stored in a desiccator for characterization assessments and adsorption tests.

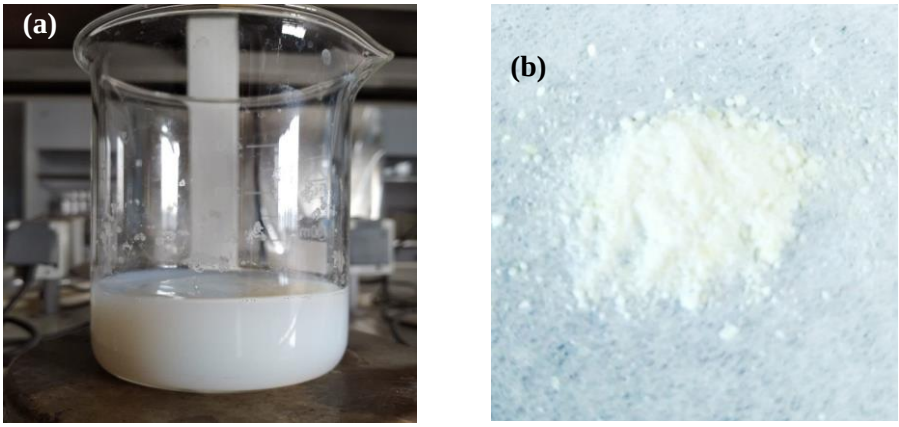

Fig. 1. (a) Milky solution obtained after mixing of $Zn(NO_3)_2$ and 2-methylimidazole solutions and (b) Synthesized ZIF-8 nanoparticles powder after centrifugation and drying.

2.3. Characterization of the synthesized adsorbent

Phase analysis and surface morphology determination of the synthesized ZIF-8 nanoparticles were done by an XRD advance diffractometer (Bruker, Germany) with Cu Kα radiation and scanning electronic microscopy (SEM –KYKY EM 3900M, China), respectively. Pore size distribution (PSD) and specific surface area assessments were performed using Barrett-Joyner-Halenda (BJH) and BET methods using a volumetric adsorption analyzer (Belsorp mini x, Japan). EDX and FTIR for elemental analysis and functional groups investigation of the synthesized adsorbent before and after adsorption were done by a field emission scanning electron microscope (KYKY-EM8000F, China) and an FT-IR imaging microscope (Bruker TENSOR II, Germany), respectively.

2.4. Adsorption tests

All adsorption tests were done at ambient temperature in the winter season (~15 ±2◦C). Initially, a solution of 100 mg. L^{-1} from Sb (III) and 100 mg. L^{-1} from Cd (II) was prepared using standard solutions of 1000 mg. L^{-1} for cadmium and

antimony. The pH of the solution was adjusted from 2 to 6 using NaOH (0.5 M) to investigate the pH effect on the removal of cadmium and antimony by ZIF-8 nanoparticles. Subsequently, 10 mg of ZIF-8 powder was poured into 10 mL of the solution and mixed for 24 minutes. Afterward, the adsorbent was separated through centrifugation (30 min, 7500 rpm) and filtration. Following the adsorption experiments, the concentration of cadmium and antimony ions was obtained by an ICP spectrometer (Perkin Elmer OPTIMA 2000, USA). The adsorption capacity (qe) and the removal percentage (R%) were determined according to Equations 1 and 2 [50]:

$$q_e(mg \cdot g^{-1}) = \frac{(C_o - C_e)}{W} V \quad (1)$$

$$R(\%) = \frac{(C_o - C_e)}{C_o} \times 100 \quad (2)$$

where C0 and Ce (mg. L^{-1}) are respectively the initial and equilibrium concentrations of metal ions, and V (mL) and W(mg) are the solution volume and adsorbent weight, respectively.

3. Results and discussion

3.1. Characterization of the ZIF-8 nanoparticles

Figure 2 shows that the size range of the synthesized nanoparticles is from 100 to 200 nm. As depicted in this figure, these nanoparticles exhibit a uniform and spherical shape. The spherical shape of nanoparticles can be attributed to the use of Zn $(NO_3)_2$ as the zinc source. According to the literature, the choice of using zinc salt, such as Zn $(OAc)_2$, Zn SO_4, Zn Cl_2, and Zn$(NO_3)_2$, can significantly impact the morphology of the prepared nanoparticles [51]. Morphology has an important role in the performance of the adsorbent. The spherical shape of the adsorbent increases access to active sites and allows for more full contact [52]. Additionally, the absorption capacity of an adsorbent to remove metal ions is more affected by its specific surface area and the abundance of active sites.

The EDX analysis elemental mapping results (Figure 3a) indicate a homogeneous distribution of the constituent elements within the ZIF-8 nanoparticles, including C, N, and Zn. The map sum spectrum (Figure 3b) demonstrates that the percentages of the C, N, and Zn elements were 64.02 wt%, 33.76 wt%, and 2.22 wt%, respectively. Figure 4a illustrates the nitrogen adsorption-desorption isotherms of the prepared nanosorbent, displaying a type IV isotherm. This indicated the presence of both microporosity and mesoporosity. The volume of pores and specific surface area of synthesized ZIF-8 nanoparticles were 117.23 $cm^3.g^{-1}$ and 510.25 $m^2.\ g^{-1}$, respectively. Furthermore, Figure 4b demonstrates a moderately wide pore size distribution (1 to 45 nm). These outcomes indicated a favorable porous structure for the synthesized adsorbent.

The ZIF-8 powder XRD pattern is shown in Figure 5. The pattern exhibited distinct peaks at positions (2θ) of 7.5, 10.5, 12.9, 14.9, 16.65, 18.23, 22.5, 24.6, 26.8,(◦), which closely aligned with the references, indicating good agreement [53].

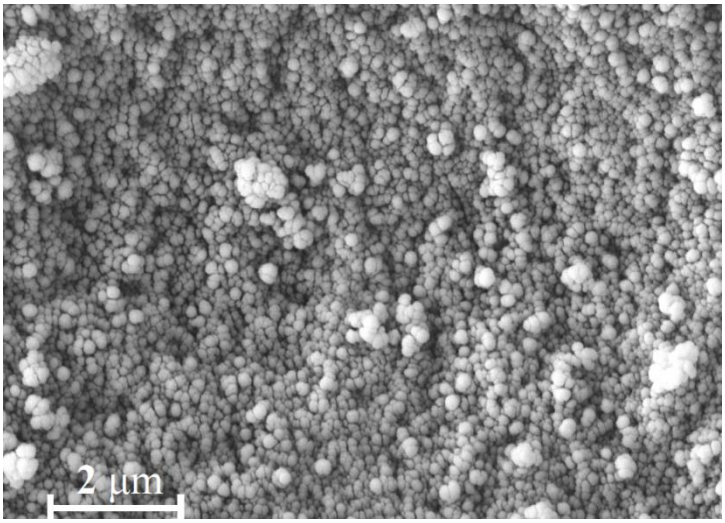

Fig. 2. FE-SEM image of synthesized ZIF-8 nanoparticles.

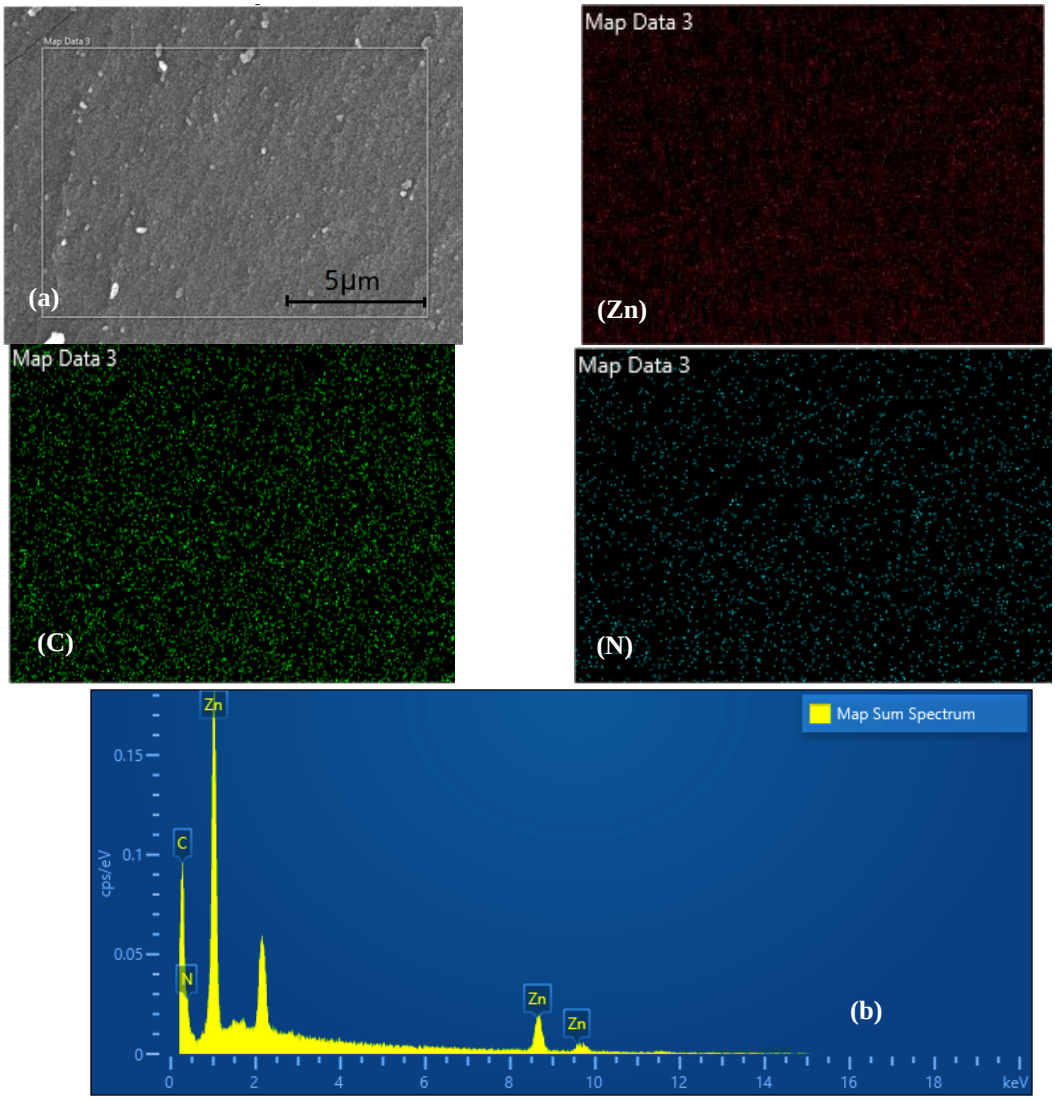

Fig. 3. (a) Elemental maps and (b) map sum spectrum of ZIF-8 nanoparticles.

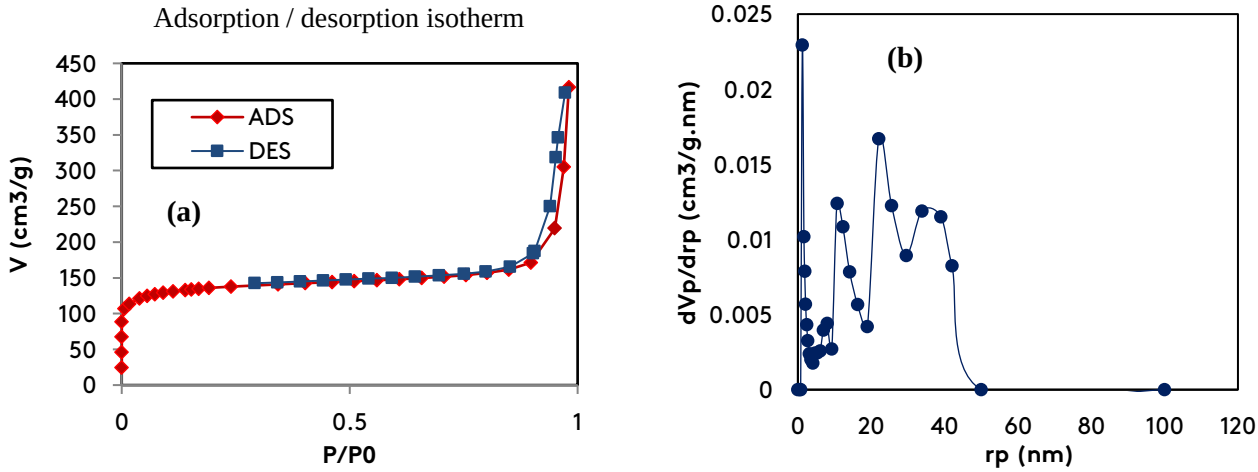

Fig. 4. (a) Adsorption-desorption isotherms of nitrogen and (b) BJH pore size distribution curve of prepared ZIF-8 nanoparticles.

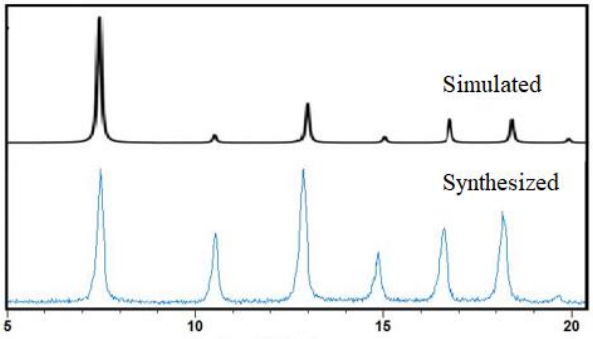

Fig. 5. XRD pattern of synthesized ZIF-8 nanoparticles.

3.2. pH effect on adsorption capacities for Cd (II) and Sb (III)

Both the solution pH and the zeta potential of the adsorbent have a substantial impact on the adsorbent's ability to adsorb metal ions. This study specifically examined the adsorption of Cd(II) and Sb(III) on ZIF-8 nanoparticles in solutions with pH values from 2 to 6. Figure 6 demonstrates that the adsorption of cadmium and antimony on the synthesized ZIF-8 nanoparticles increased as the pH of the solution was raised from 2 to 6.

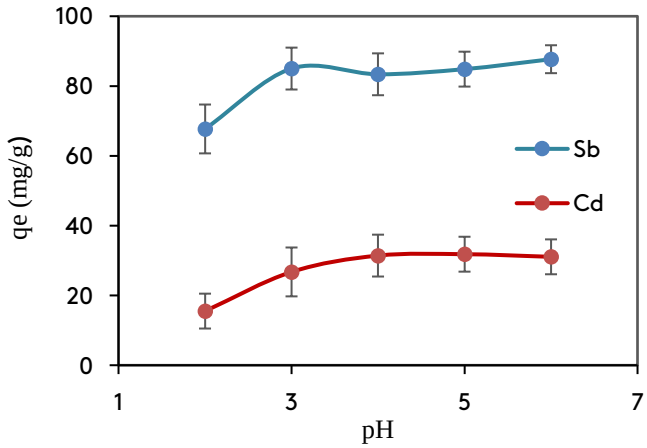

Fig. 6. pH effect of the solution on the adsorption capacity of prepared nanosorbent for the antimony and cadmium removal. (T= 15 ±2 ◦C, adsorbent dose =100 mg. L^{-1}, the concentration of ions =100 mg. L^{-1}).

Numerous studies have examined the pH influence of the solution on the adsorption capacity of various adsorbents for different metal ions [54-56]. These studies have demonstrated that the pH effect on adsorption capacity is multifaceted, relying on factors such as the adsorbent's surface pH IEP and the specific metal species available in the solution at different pH values. Notably, the isoelectric pH of ZIF-8 nanoparticles is approximately 9.6 [41]. However, due to the precipitation of cadmium at pH values above 6, investigating the impact of solution pH beyond the isoelectric point was not feasible in this study. Below the isoelectric point, the ZIF-8 surface carries a positive charge. As pH increases and approaches the isoelectric point (pH 9.6), the positive charge of the surface diminishes. This reduction in positive charge enhances the electrostatic attraction between the surface and the positive ions of Cd(II) and Sb(III), thereby increasing the adsorption capacity. Similar findings have been reported in the literature [23]. It is necessary to mention that in some cases, the adsorption capacity decreases with increasing pH below the isoelectric point. This occurs when negatively charged species of ions are present in aqueous solutions at low pH values. For instance, arsenic ion (As(V)) exists as H_2AsO_4- in aqueous solutions at pH values below 7. The negative charge of this arsenic species results in increased electrostatic repulsion between the adsorbent surface and the arsenic ion species as the solution pH rises and the adsorbent zeta potential decreases.

Consequently, the adsorption capacity decreases [57]. Given that cadmium and antimony ions precipitate at pH values higher than the ZIF-8 isoelectric point, their adsorption rate was investigated at a pH below the isoelectric point. The results indicated that the synthesized adsorbent exhibited the highest adsorption capacity at a neutral pH of 6. This is advantageous for water purification purposes, particularly in

natural waters and drinking water, which typically have a neutral pH. The ability of an adsorbent to maintain high adsorption capacity within the neutral pH range is considered favorable, as it eliminates the need to adjust the pH of the water. Additionally, Figure 6 highlights the superior performance of the synthesized adsorbent in the uptake of antimony ions compared to cadmium ions. This discrepancy in adsorption capacity could be attributed to the ionic radius of Sb(III) being smaller in comparison to Cd(II) and also its electronegativity being higher than Cd(II). The values of ionic radius and electronegativity for these metals are provided in Table 1.

Table 1. Ionic radius and electronegativity values for Cd and Sb.

Element	Ionic radius (pm)	Electronegativity
Cd	95	1.69
Sb	75	2.05

The FTIR spectrum (Figure 7) was applied to assess the functional groups of the ZIF-8 nanoparticles both before and after the uptake of Cd(II) and Sb(III). The diffraction peak at 1456.72 cm^{-1} in ZIF-8 spectrums (Figure 7a) was related to the C=C bonds. Peaks at 2927 cm^{-1} were attributed to the stretching vibration of the benzene ring C–H bonds. The diffraction peak at 1571.89 cm^{-1} was the stretching vibration adsorption bonds of the C=O. As observed in Figure 7b, the peak at 1571.89 cm^{-1} (C=O groups) shifted to 1573.15 cm^{-1} and became broader. Additionally, new peaks within the range of 500 to 900 cm^{-1} emerged, demonstrating the adsorption of Cd (II) and Sb (III) ions onto the ZIF-8 nanoparticles.

3.3. Adsorption kinetics

The adsorption capacity of ZIF-8 nanoparticles was evaluated using kinetic models. In summary, the simple linear expressions of these models are presented in the following equations.

$$\ln(q_e - q_t) = \ln q_e - k_1 t \quad \text{pseudo-first-order} \quad (3)$$

$$\frac{t}{q_t} = \frac{1}{k_2 q_e^2} + \frac{t}{q_e} \quad \text{pseudo-second-order} \quad (4)$$

$$q_t = k_p t^{\frac{1}{2}} + C \quad \text{intra-particle diffusion} \quad (5)$$

where qe (mg. g^{-1}) is the amount of removed antimony and cadmium ions per gram of adsorbent at equilibrium and qt (mg. g^{-1}) is the amount of adsorbed antimony and cadmium ions per gram of adsorbent at various times. Also, k1(min^{-1}) and k2 ($g.mg^{-1}.min^{-1}$) are adsorption rate constants for pseudo-first-order and pseudo-second-order kinetics, respectively. In the intra-particle diffusion model, kp ($mg.g^{-1}.min^{-1/2}$) is the model constant [58]. Figure 8 shows diagrams of the pseudo-first-order, pseudo-second-order, and intra-particle diffusion kinetic models for antimony and cadmium adsorption on synthesized ZIF-8 nanoparticles.

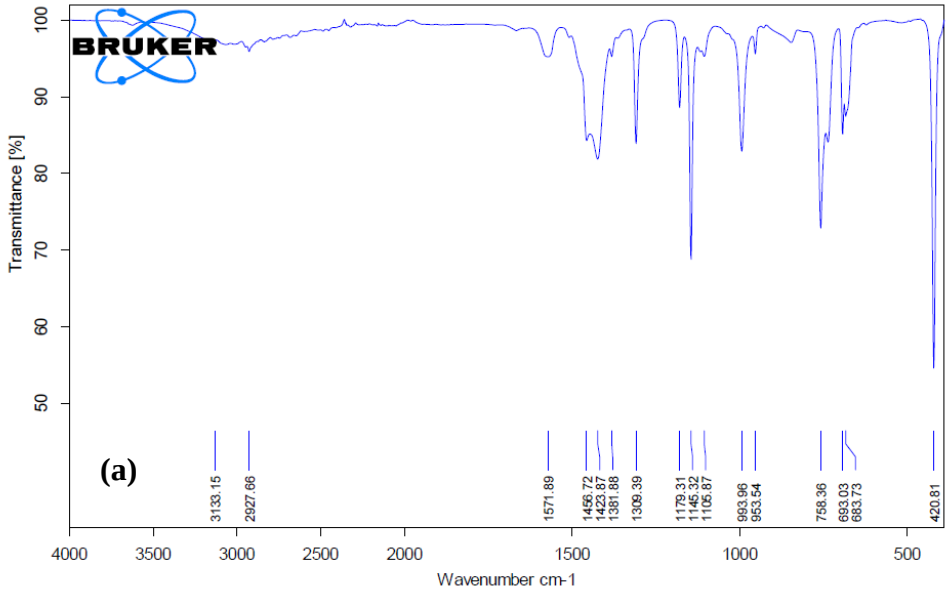

Fig. 7. FTIR spectra of ZIF-8 a) before and b) after adsorption of Cd (II) and Sb (III) ions.

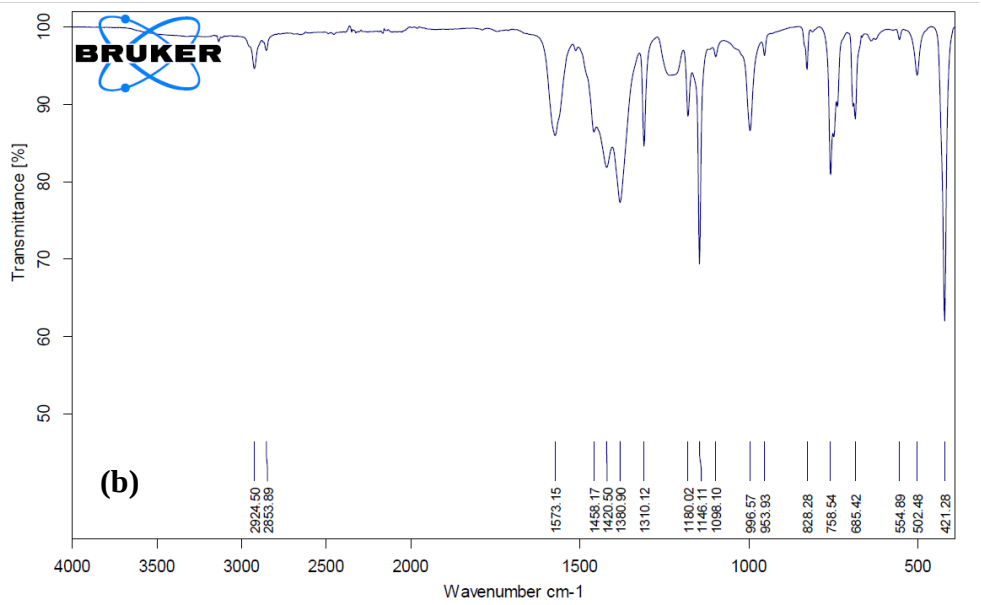

Fig. 7. (Continued) FTIR spectra of ZIF-8 a) before and b) after adsorption of Cd (II) and Sb (III) ions.

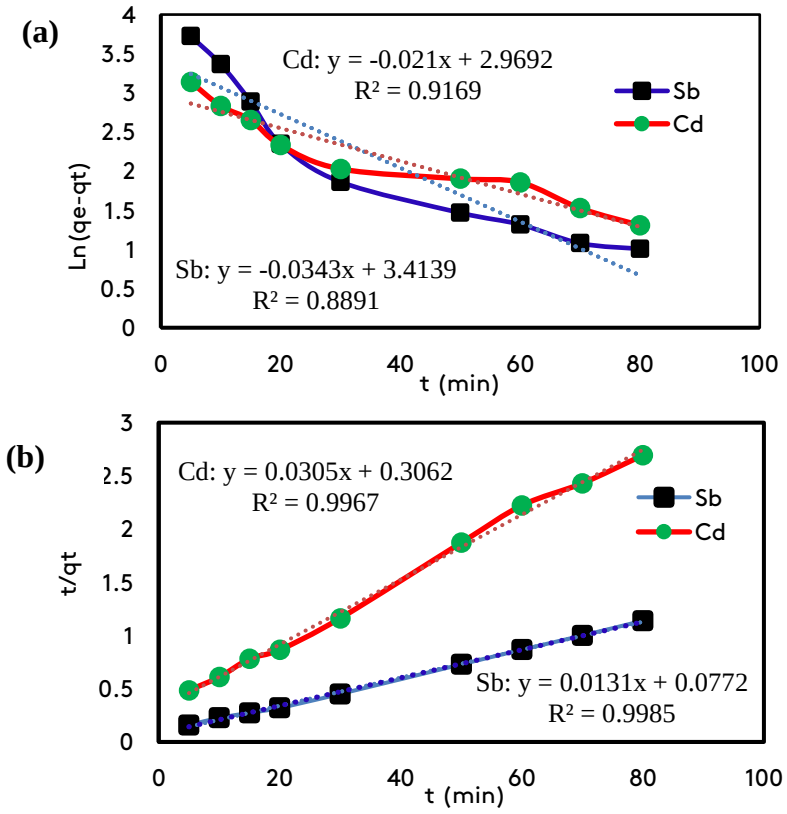

Fig. 8. Pseudo-first-order (a), pseudo-second-order (b), and intra-particle diffusion kinetics (c) sorption diagrams for the Sb (III) and Cd (II) removal by ZIF-8 nanoparticles.

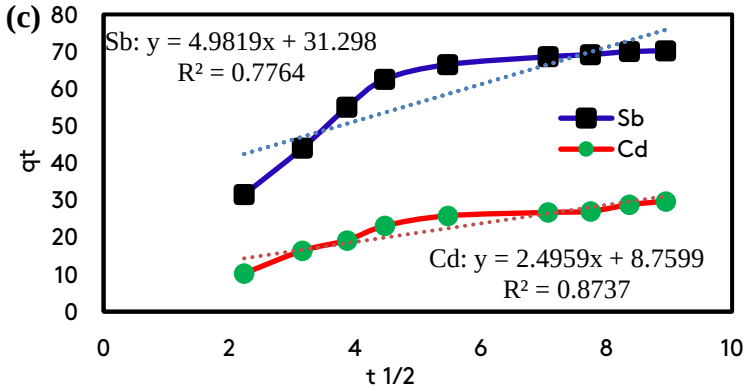

Fig. 8. (Continued) Pseudo-first-order (a), pseudo-second-order (b), and intra-particle diffusion kinetics (c) sorption diagrams for the Sb (III) and Cd (II) removal by ZIF-8 nanoparticles.

The kinetic data demonstrated that the correlation coefficients (R2) for both Cd (II) and Sb (III) in the pseudo-second-order kinetics were closer to one compared to the pseudo-first-order kinetics (Table 2). This observation revealed that the step of rate-controlling in the removal of Cd and Sb was the chemical interaction between the metal ions and the ZIF-8 functional groups.

3.4. Adsorption thermodynamic

The adsorption of Sb (III) and Cd (II) on ZIF-8 was examined at several temperatures (298 to 318 K) to determine the thermodynamic manner governing the system from the point of physical or chemical adsorption view. Thermodynamic parameters of the enthalpy change (ΔH°), the standard Gibbs free energy (ΔG°), and entropy change (ΔS°) were obtained using Equations 6 and 7 [59].

$$\Delta G^\circ = \Delta H^\circ - T\Delta S^\circ \quad (6)$$

$$\ln K_c = \frac{\Delta S^\circ}{R} - \frac{\Delta H^\circ}{RT} \quad (7)$$

where R= 8.314 J.mol^{-1}. K^{-1} is the universal gas constant, T (K) is the studied temperature, and Kc (Kc = qe/Ce) is the equilibrium constant.

The ΔH° and ΔS° values were obtained using the intercept and slope determined from plotting Ln Kc versus 1/T (Figure 9). The thermodynamic factors are presented in Table 3.

Table 2. Parameters of the kinetic models for Cd (II) and Sb (III) adsorbed by ZIF-8 nanoparticles.

Kinetic models	Pseudo-first-order			Pseudo-second-order			Intra-particle diffusion		
Parameters	$q_e(\frac{mg}{g})$	$k_1(\frac{1}{min})$	R^2	$q_e(\frac{mg}{g})$	$k_2(\frac{g}{mg.min})$	R^2	$k_p\ (\frac{mg}{g.min^{\frac{1}{2}}})$	$C(\frac{mg}{g})$	R^2
Sb	30.38	0.0343	0.917	76.33	0.0022	0.9985	4.982	31.298	0.7764
Cd	19.48	0.021	0.889	32.79	0.003	0.9967	2.4959	8.7599	0.8737

Table 3. Thermodynamic parameters for Sb (III) and Cd (II) adsorption using ZIF-8 nanoparticles.

Materials	$\Delta G^\circ(\frac{J}{mol})$			$\Delta H^\circ(\frac{J}{mol})$	$\Delta S^\circ(\frac{J}{mol.K})$
	at: 298 K	308 K	318 K		
Sb	- 1884	-2052	-2220	+3126.9	+16.817
Cd	- 1666	-1852	-2038	+3886.2	+18.632

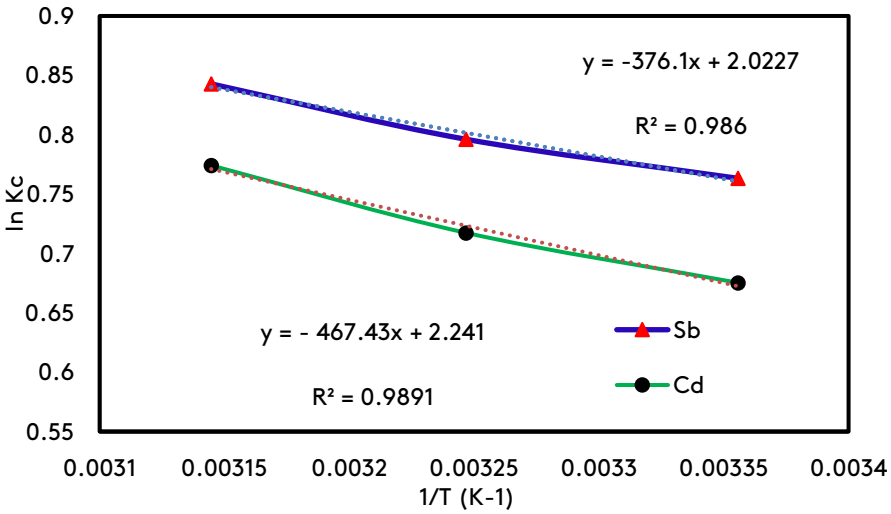

Fig. 9. Plot of Ln K_c versus 1/T for the adsorption of Sb (III) and Cd (II) by ZIF-8 nanoparticles. (adsorbent dose =100 mg. L^{-1}, the concentration of ions =100 mg. L^{-1}, pH = 6, and t = 1 h).

The negative values of Gibbs free energies within the studied temperature range indicated that the uptake of Sb(III) and Cd(II) by the synthesized ZIF-8 nanoparticles was a spontaneous process. Additionally, the ΔH° positive value suggested that the adsorption was an endothermic process [54]. Furthermore, the ΔS° positive value indicated the degree of randomness in the solid/liquid interactions increased within the adsorption process of antimony and cadmium on ZIF-8.

3.5. Performance of other adsorbents

The maximum adsorption capacity of synthesized ZIF-8 nanoparticles was obtained at 31.8 and 87.68 mg of metal per gram of adsorbent for Cd (II) and Sb (III), respectively. Comparing the adsorption capacity results of other adsorbents (Table 4) showed the adsorption capacity of synthesized ZIF-8 nanoparticles for Cd (II) removal was higher than many adsorbents [60, 61] and carbon nanotubes [29]. Table 4 shows that the adsorption capacity of prepared nanosorbent for Sb (III) uptake was also higher than many adsorbents such as UiO- 66 (NH2) [24], GAD beads [62] and swine manure pyrochar [63]. The latest studies show that the only adsorbent that has performed the simultaneous adsorption of Sb (III) and Cd (II) with a higher adsorption capacity than the adsorbent synthesized in this work was a composite of biochar and Fe/Mn oxides [32, 64]. This suggested that the incorporation of Fe/Mn oxide nanoparticles onto the biochar surfaces significantly enhanced the uptake of Sb(III).

The synthesis of the adsorbent used in this study is a straightforward process that can be carried out at ambient temperature and pressure using an inexpensive and non-toxic solvent. The maximum adsorption capacity of this adsorbent is achieved at a neutral pH (pH 6), which is similar to the conditions found in natural waters, particularly drinking water.

4. Conclusions

Heavy metals pose a significant threat as environmental pollutants. Utilizing adsorbents prepared through convenient and environmentally friendly methods can greatly enhance the efficiency of heavy metal adsorption. In this study, ZIF-8 nanoparticles were prepared under ambient conditions using water as a non-toxic solvent. These environmentally friendly MOFs were employed for the simultaneous adsorption of cadmium and antimony from aqueous solutions. The adsorbent exhibited a maximum adsorption capacity of 31.8 mg. g^{-1} for cadmium and 87.68 mg. g^{-1} for antimony, both achieved at a pH of 6. The results demonstrated that the prepared adsorbent has substantial potential for efficiently removing heavy metals, particularly cadmium and antimony, from wastewater.

Table 4. Comparison of the adsorption capacity of various adsorbents for Sb (III) and Cd (II) removal from water solution.

Adsorbent	q_{max} ($mg.g^{-1}$)		pH	Initial Concentration ($mg.L^{-1}$)	Ref.
	Sb (III)	Cd (II)			
Sugarcane bagasse alginate porous gel beads	-	176.36	5.5	150-300	[65]
UiO- 66 (NH_2)	61.8	-	1.5	10-600	[24]
Lucerne biochar	-	6.28	5.5	0.58-2.28	[60]
Fe-Mn binary oxide	101	-	3	25-250	[66]
GAD beads	7.67	-	6	220	[62]
Bamboo charcoal	-	12.08	>8	50	[61]
Fe_3O_4@ZIF-8	-	370	6	10-100	[23]
Fe_3O_4@APS@AA-co-CA MNPs	-	29.6	5.5	20-450	[67]
Pyrochar from swine manure	13.09	81.32	6	0.3-150 (for Cd) 0.1-100 (for Sb)	[63]
Magnetic carbon nanotubes	-	17.9	6	3-30	[29]
$MnFe_2O_4$–BC	237.53	181.49	7	25-500	[32]
Fe-Mn binary oxide /bone char	209.0	48.8	2-7	10	[64]
ZIF-8 nanoparticles	87.68	31.8	6	100	This study

Acknowledgements

The authors sincerely thank all those who helped in conducting this research, especially the personnel of the central laboratory of Sistan and Baluchistan University.

Declaration of competing interest

The authors declare that they have no known competing financial interests or personal relationships that would influence this paper.

References

[1] Moghadam, H. and Samimi, M. (2022). Effect of condenser geometrical feature on evacuated tube collector basin solar still performance: productivity optimization using a Box-Behnken design model. Desalination, 542116092. https://doi.org/10.1016/j.desal.2022.116092

[2] Samimi, M. and Moghadam, H. (2024). Investigation of structural parameters for inclined weir-type solar stills. Renewable and Sustainable Energy Reviews, 190113969. https://doi.org/10.1016/j.rser.2023.113969

[3] Samimi, M. (2024). Efficient biosorption of cadmium by Eucalyptus globulus fruit biomass using process parameters optimization. Global Journal of Environmental Science and Management, 10(1), 27-38. https://doi.org/10.22034/gjesm.2024.01.03

[4] Qasem, N.A.A., Mohammed, R.H., and Lawal, D.U. (2021). Removal of heavy metal ions from wastewater: a comprehensive and critical review. npj Clean Water 4:361-15. https://doi.org/10.1038/s41545-021-00127-0

[5] Wang, K., Tian, Z., and Yin, N. (2018). Significantly enhancing Cu (II) adsorption onto Zr-MOFs through Novel cross-flow disturbance of ceramic membrane. Industrial & Engineering Chemistry Research 1-32. https://doi.org/10.1021/acs.iecr.7b04850

[6] Liu, B., Kim, K. H., Kumar, V., & Kim, S. (2020). A review of functional sorbents for adsorptive removal of arsenic ions in aqueous systems. Journal of hazardous materials, 388, 121815. https://doi.org/10.1016/j.jhazmat.2019.121815

[7] Levio-Raiman, M., Briceño, G., Schalchli, H., Bornhardt, C., & Diez, M. C. (2021). Alternative treatment for metal ions removal from acid mine drainage using an organic biomixture as a low cost adsorbent. Environmental Technology & Innovation, 24, 101853. https://doi.org/10.1016/j.eti.2021.101853

[8] Simate, G.S. and Ndlovu, S. (2014). Acid mine drainage: Challenges and opportunities. Journal of Environmental Chemical Engineering, 1785-1803. https://doi.org/10.1016/j.jece.2014.07.021

[9] Tong, L., Fan, R., Yang, S., & Li, C. (2021). Development and status of the treatment

technology for acid mine drainage. Mining, Metallurgy & Exploration, 38, 315-327. https://doi.org/10.1007/s42461-020-00298-3

[10] Asghar, A., Bello, M. M., & Raman, A. A. A. (2021). Metal-organic frameworks for heavy metal removal. Applied Water Science: Remediation Technologies, 2, 321-356. https://doi.org/10.1002/9781119725282.ch9

[11] Türksoy, R., Terzioğlu, G., Yalçın, İ. E., Türksoy, Ö., & Demir, G. (2021). Removal of heavy metals from textile industry wastewater. Frontiers in Life Sciences and Related Technologies, 2(2), 44-50. https://doi.org/10.51753/flsrt.958165

[12] Azanaw, A., Birlie, B., Teshome, B., & Jemberie, M. (2022). Textile effluent treatment methods and eco-friendly resolution of textile wastewater. Case Studies in Chemical and Environmental Engineering, 6, 100230. https://doi.org/10.1016/j.cscee.2022.100230

[13] Hansen, E., Aquim, P.M.d., and Gutterres, M. (2021). Current technologies for post-tanning wastewater treatment: A review Journal of Environmental Management, 294113003. https://doi.org/10.1016/j.jenvman.2021.113003

[14] Zhao, J., Wu, Q., Tang, Y., Zhou, J., & Guo, H. (2022). Tannery wastewater treatment: conventional and promising processes, an updated 20-year review. Journal of Leather Science and Engineering, 4(1), 10. https://doi.org/10.1186/s42825-022-00082-7

[15] Navin, P.K., Kumar, S., and Mathur, M. (2018). Textile wastewater treatment: a critical review. International Journal of Engineering Research & Technology, 6(11), 1-7. https://doi.org/ 10.17577/IJERTCONV6IS11015

[16] Samimi, M. and Shahriari-Moghadam, M. (2023). The Lantana camara L. stem biomass as an inexpensive and efficient biosorbent for the adsorptive removal of malachite green from aquatic environments: kinetics, equilibrium and thermodynamic studies. International Journal of Phytoremediation, 25(10), 1328-1336. https://doi.org/10.1080/15226514.2022.2156978

[17] Zhang, S., Wang, J., Zhang, Y., Ma, J., Huang, L., Yu, S., ... & Wang, X. (2021). Applications of water-stable metal-organic frameworks in the removal of water pollutants: A review. Environmental Pollution, 291, 118076. https://doi.org/10.1016/j.envpol.2021.118076

[18] Samimi, M. and Nouri, J. (2023). Optimized Zinc Uptake from the Aquatic Environment Using Biomass Derived from Lantana Camara L. Stem. Pollution, 9(4), 1925-1934. https://doi.org/10.22059/poll.2023.363363.2014

[19] Kastury, F., Besedin, J., Betts, A. R., Asamoah, R., Herde, C., Netherway, P., ... & Juhasz, A. L. (2024). Arsenic, cadmium, lead, antimony bioaccessibility and relative bioavailability in legacy gold mining waste. Journal of hazardous materials, 469, 133948. https://doi.org/10.1016/j.jhazmat.2024.133948

[20] Zhou, S., Hursthouse, A., and Chen, T. (2019). Pollution Characteristics of Sb, As, Hg, Pb, Cd, and Zn in Soils from Different Zones of Xikuangshan Antimony Mine. Journal of Analytical Methods in Chemistry, 21-9. https://doi.org/10.1155/2019/2754385

[21] Mansoorianfar, M., Nabipour, H., Pahlevani, F., Zhao, Y., Hussain, Z., Hojjati-Najafabadi, A., ... & Pei, R. (2022). Recent progress on adsorption of cadmium ions from water systems using metal-organic frameworks (MOFs) as an efficient class of porous materials. Environmental Research, 214, 114113. https://doi.org/10.1016/j.envres.2022.114113

[22] Mirshrkari, S., Shojaei, V., and Khoshdast, H. (2022). Adsorptive Study of Cadmium Removal from Aqueous Solution Using a Coal Waste Loaded with Fe_3O_4 Nanoparticles. International Journal of Mining, Reclamation and Environment, 13527-545. https://doi.org/10.22044/jme.2022.11796.2174

[23] Abdel-Magied, A. F., Abdelhamid, H. N., Ashour, R. M., Fu, L., Dowaidar, M., Xia, W., & Forsberg, K. (2022). Magnetic metal-organic frameworks for efficient removal of cadmium (II), and lead (II) from aqueous solution. Journal of Environmental Chemical Engineering, 10(3), 107467. https://doi.org/10.1016/j.jece.2022.107467

[24] He, X., Min, X., and Luo, X. (2017). Efficient Removal of Antimony (III, V) from Contaminated Water by Amino Modification of a Zirconium Metal–Organic Framework with

Mechanism Study. Journal of Chemical & Engineering Data, 62 1519-1529. https://doi.org/10.1021/acs.jced.7b00010

[25] Bolisetty, S., Peydayesh, M., and Mezzenga, R. (2019). Sustainable technologies for water purification from heavy metals: review and analysis. Chemical Society Reviews, 48463-487. https://doi.org/10.1039/c8cs00493e

[26] Kumar, V. and Dwivedi, S.K. (2021). Mycoremediation of heavy metals: processes, mechanisms, and affecting factors. RSC Advances, 2810375-10412. https://doi.org/10.1007/s11356-020-11491-8

[27] Samimi, M., Mohammadzadeh, E., and Mohammadzadeh, A. (2023). Rate enhancement of plant growth using Ormus solution: optimization of operating factors by response surface methodology. International Journal of Phytoremediation, 25(12), 1636–1642. https://doi.org/10.1080/15226514.2023.2179014

[28] Arora, R. (2019). Adsorption of Heavy Metals–A Review. Materials Today, 184745-4750. https://doi.org/10.1016/j.matpr.2019.07.462

[29] El-Sheikh, A. H., Alahmad, F. A., Sunjuk, M. S., & Al-Hashimi, N. N. (2022). Cd (II) removal from phenols-bearing wastewater using magnetic carbon nanotubes. Emerging Contaminants, 8, 400-410. https://doi.org/10.1016/j.emcon.2022.11.001

[30] Jadoun, S., Fuentes, J. P., Urbano, B. F., & Yáñez, J. (2023). A review on adsorption of heavy metals from wastewater using conducting polymer-based materials. Journal of Environmental Chemical Engineering, 11(1), 109226. https://doi.org/10.1016/j.jece.2022.109226

[31] Moghadam, H., Zakeri, M., and Samimi, A. (2019). Optimization of calcium alginate beads production by electrospray using response surface methodology. Materials Research Express 6 https://doi.org/10.1088/2053-1591/ab3377

[32] Wang, Y. Y., Ji, H. Y., Lu, H. H., Liu, Y. X., Yang, R. Q., He, L. L., & Yang, S. M. (2018). Simultaneous removal of Sb (III) and Cd (II) in water by adsorption onto a MnFe 2 O 4–biochar nanocomposite. RSC advances, 8(6), 3264-3273. https://doi.org/10.1039/C7RA13151H

[33] Moghadam, H., Samimi, A., and Behzadmehr, A. (2013). Effect of Nanoporous Anodic Aluminum Oxide (AAO) Characteristics On Solar Absorptivity. Challenges in Nano and Micro Scale Science and Technology, 1(2), 110-116. https://doi.org/10.7508/tpnms.2013.02.004

[34] Karnib, M., Kabbani, A., Holail, H., & Olama, Z. (2014). Heavy metals removal using activated carbon, silica and silica activated carbon composite. Energy Procedia, 50, 113-120. https://doi.org/10.1016/j.egypro.2014.06.014

[35] Ehzari, H., Amiri, M., Safari, M., & Samimi, M. (2022). Zn-based metal-organic frameworks and p-aminobenzoic acid for electrochemical sensing of copper ions in milk and milk powder samples. International Journal of Environmental Analytical Chemistry, 102(16), 4364-4377. https://doi.org/10.1080/03067319.2020.1784410

[36] Kaur, H., Devi, N., Siwal, S. S., Alsanie, W. F., Thakur, M. K., & Thakur, V. K. (2023). Metal–organic framework-based materials for wastewater treatment: superior adsorbent materials for the removal of hazardous pollutants. ACS omega, 8(10), 9004-9030. https://doi.org/10.1021/acsomega.2c07719

[37] Jian, X. and He, B.X. (2019). Recent advances about metal-organic frameworks in the removal of pollutants from wastewater. Coordination Chemistry Reviews, 37817-31. https://doi.org/10.1016/j.ccr.2018.03.015

[38] Ehzari, H., Safari, M., and Samimi, M. (2021). Signal amplification of novel sandwich-type genosensor via catalytic redox-recycling on platform MWCNTs/Fe_3O_4@ TMU-21 for BRCA1 gene detection. Talanta, 234122698. https://doi.org/10.1016/j.talanta.2021.122698

[39] Li, K., Miwornunyuie, N., Chen, L., Jingyu, H., Amaniampong, P. S., Ato Koomson, D., ... & Lu, H. (2021). Sustainable application of ZIF-8 for heavy-metal removal in aqueous solutions. Sustainability, 13(2), 984. https://doi.org/10.3390/su13020984

[40] Shahsavari, M., Mohammadzadeh Jahani, P., Sheikhshoaie, I., Tajik, S., Aghaei Afshar, A., Askari, M. B., ... & Beitollahi, H. (2022). Green synthesis of zeolitic imidazolate frameworks: a review of their characterization and industrial and medical applications. Materials, 15(2), 447. https://doi.org/10.3390/ma15020447

[41] Jian, M., Liu, B., Zhang, G., Liu, R., & Zhang, X. (2015). Adsorptive removal of arsenic from aqueous solution by zeolitic imidazolate framework-8 (ZIF-8) nanoparticles. Colloids and Surfaces A: Physicochemical and Engineering Aspects, 465, 67-76. https://doi.org/10.1016/j.colsurfa.2014.10.023

[42] Liu, B., Jian, M., Wang, H., Zhang, G., Liu, R., Zhang, X., & Qu, J. (2018). Comparing adsorption of arsenic and antimony from single-solute and bi-solute aqueous systems onto ZIF-8. Colloids and Surfaces A: Physicochemical and Engineering Aspects, 538, 164-172. https://doi.org/10.1016/j.colsurfa.2017.10.068

[43] Ahmad, S. Z. N., Salleh, W. N. W., Yusof, N., Yusop, M. Z. M., Hamdan, R., & Ismail, A. F. (2023). Synthesis of zeolitic imidazolate framework-8 (ZIF-8) using different solvents for lead and cadmium adsorption. Applied Nanoscience, 13(6), 4005-4019. https://doi.org/10.1007/s13204-022-02680-7

[44] Roostan, Z., Rashidi, A., and Borghei, S.M. (2018). Nickel ion removal from aqueous solution using recyclable zeolitic imidazolate framework-8 (ZIF-8) nano adsorbent: a kinetic and equilibrium study. Desalination and Water Treatment, 103141–151. https://doi.org/10.5004/dwt.2018.21811

[45] Zhou, L., Li, N., Owens, G., & Chen, Z. (2019). Simultaneous removal of mixed contaminants, copper and norfloxacin, from aqueous solution by ZIF-8. Chemical engineering journal, 362, 628-637. https://doi.org/10.1016/j.cej.2019.01.068

[46] Li, D. and Xu, F. (2021). Removal of Cu (II) from aqueous solutions using ZIF-8@GO composites. Journal of Solid State Chemistry, 302122406. https://doi.org/10.1016/j.jssc.2021.122406

[47] Shahrak, M.N., Ghahramaninezhad, M., and Eydifarash, M. (2017). Zeolitic imidazolate framework-8 for efficient adsorption and removal of Cr(VI) ions from aqueous solution. Environmental Science and Pollution Research, 249624-9634. https://doi.org/10.1021/am403079n

[48] Hu, L., Zhang, P., Hu, Q., Huang, Y., Li, J., Pei, X., ... & Yu, D. (2024). Synthesis of ZIF-8 in high yield and simultaneous removal of Mn (II), Cu (II), and Cd (II): performance and mechanism. Chemical Engineering Research and Design. https://doi.org/10.1016/j.cherd.2024.06.022

[49] Yin, L., Li, W., Lin, S., Owens, G., & Chen, Z. (2022). Simultaneous removal of arsenite and arsenate from mining wastewater using ZIF-8 embedded with iron nanoparticles. Chemosphere, 304, 135269. https://doi.org/10.1016/j.chemosphere.2022.135269

[50] Samimi, M. and Moeini, S. (2020). Optimization of the Ba+ 2 uptake in the formation process of hydrogels using central composite design: Kinetics and thermodynamic studies of malachite green removal by Ba-alginate particles. Journal of Particle Science and Technology, 6(2), 95-102. https://doi.org/ 10.22104/jpst.2021.4842.1184

[51] Jian, M., Liu, B., Liu, R., Qu, J., Wang, H., & Zhang, X. (2015). Water-based synthesis of zeolitic imidazolate framework-8 with high morphology level at room temperature. Rsc Advances, 5(60), 48433-48441. https://doi.org/10.1039/C5RA04033G

[52] Dai, J., Xiao, S., Liu, J., He, J., Lei, J., & Wang, L. (2017). Fabrication of ZIF-9@ super-macroporous microsphere for adsorptive removal of Congo red from water. Rsc Advances, 7(11), 6288-6296. https://doi.org/10.1039/C6RA26763G

[53] Karagiaridi, O., Lalonde, M. B., Bury, W., Sarjeant, A. A., Farha, O. K., & Hupp, J. T. (2012). Opening ZIF-8: a catalytically active zeolitic imidazolate framework of sodalite topology with unsubstituted linkers. Journal of the American Chemical Society, 134(45), 18790-18796. https://doi.org/10.1021/ja308786r

[54] Samimi, M., Zakeri, M., Alobaid, F., & Aghel, B. (2022). A brief review of recent results in arsenic adsorption process from aquatic environments by metal-organic frameworks: classification based on kinetics, isotherms and thermodynamics behaviors. Nanomaterials, 13(1), 60. https://doi.org/10.3390/nano13010060

[55] Laus, R., Costa, T. G., Szpoganicz, B., & Fávere, V. T. (2010). Adsorption and desorption of Cu (II), Cd (II) and Pb (II) ions using chitosan crosslinked with epichlorohydrin-triphosphate as the adsorbent. Journal of hazardous materials, 183(1-3), 233-241. https://doi.org/10.1016/j.jhazmat.2010.07.016

[56] Yin, N., Wang, K., & Li, Z. (2018). Novel melamine modified metal-organic frameworks for remarkably high removal of heavy metal Pb (II). Desalination, 430, 120-127. https://doi.org/10.1016/j.desal.2017.12.057

[57] Sun, J., Zhang, X., Zhang, A., & Liao, C. (2019). Preparation of Fe–Co based MOF-74 and its effective adsorption of arsenic from aqueous solution. Journal of Environmental Sciences, 80, 197-207. https://doi.org/10.1016/j.jes.2018.12.013

[58] Samimi, M. and Shahriari-Moghadam, M. (2021). Isolation and identification of Delftia lacustris Strain-MS_3 as a novel and efficient adsorbent for lead biosorption: Kinetics and thermodynamic studies, optimization of operating variables. Biochemical Engineering Journal 173 https://doi.org/10.1016/j.bej.2021.108091

[59] Samimi, M. and Safari, M. (2022). TMU-24 (Zn-based MOF) as an advance and recyclable adsorbent for the efficient removal of eosin B: Characterization, equilibrium, and thermodynamic studies. Environmental Progress & Sustainable Energy 4113859. https://doi.org/10.1002/ep.13859

[60] Bandara, T., Xu, J., Potter, I. D., Franks, A., Chathurika, J. B. A. J., & Tang, C. (2020). Mechanisms for the removal of Cd (II) and Cu (II) from aqueous solution and mine water by biochars derived from agricultural wastes. Chemosphere, 254, 126745. https://doi.org/10.1016/j.chemosphere.2020.126745

[61] Wang, F.Y., Wang, H., and Ma, J.W. (2010). Adsorption of cadmium (II) ions from aqueous solution by a new low-cost adsorbent—Bamboo charcoal. Journal of Hazardous Materials, 177300-306. https://doi.org/10.1016/j.jhazmat.2009.12.032

[62] Yang, X., Zhou, T., Deng, R., Zhu, Z., Saleem, A., & Zhang, Y. (2021). Removal of Sb (III) by 3D-reduced graphene oxide/sodium alginate double-network composites from an aqueous batch and fixed-bed system. Scientific Reports, 11(1), 22374. https://doi.org/10.1038/s41598-021-01788-0

[63] Han, L., Sun, H., Ro, K. S., Sun, K., Libra, J. A., & Xing, B. (2017). Removal of antimony (III) and cadmium (II) from aqueous solution using animal manure-derived hydrochars and pyrochars. Bioresource Technology, 234, 77-85. https://doi.org/10.1016/j.biortech.2017.02.130

[64] Han, X., Cheng, C., Zhang, W., Li, S., Jia, Q., & Xiu, G. (2023). Performance and mechanism of simultaneous Sb (III) and Cd (II) removal from water by Fe–Mn binary oxide/bone char. Environmental Science and Pollution Research, 30(35), 84437-84451. https://doi.org/10.1007/s11356-023-27832-2

[65] Fan, S., Zhou, J., Zhang, Y., Feng, Z., Hu, H., Huang, Z., & Qin, Y. (2020). Preparation of sugarcane bagasse succinate/alginate porous gel beads via a self-assembly strategy: Improving the structural stability and adsorption efficiency for heavy metal ions. Bioresource technology, 306, 123128. https://doi.org/10.1016/j.biortech.2020.123128

[66] Xu, W., Wang, H., Liu, R., Zhao, X., & Qu, J. (2011). The mechanism of antimony (III) removal and its reactions on the surfaces of Fe–Mn binary oxide. Journal of colloid and interface science, 363(1), 320-326. https://doi.org/10.1016/j.jcis.2011.07.026

[67] Ge, F., Li, M. M., Ye, H., & Zhao, B. X. (2012). Effective removal of heavy metal ions Cd^{2+}, Zn^{2+}, Pb^{2+}, Cu^{2+} from aqueous solution by polymer-modified magnetic nanoparticles. Journal of hazardous materials, 211, 366-372. https://doi.org/10.1016/j.jhazmat.2011.12.013

How to cite this paper:

Soltani, P., Zakeri, M., Samimi, A. & Agah, A. (2025). Green synthesis of ZIF-8 nanoparticles for the simultaneous removal of Cd (II) and Sb (III) from contaminated wastewater. Advances in Environmental Technology, 11(1), 75-90. DOI: 10.22104/aet.2024.6938.1901